18. J.K. Chen, C.T. Sun, and C.I. Chang. 1985. "Failure Analysis of a Graphite/Epoxy Laminate Subjected to Combined Thermal and Mechanical Loading," *J. Composite Mater.*, 19: 408–423.
19. J.J. Schubbe and S. Mall. 1991. "Damage Mechanisms in a Cross-Ply Metal Matrix Composite Under Thermal-Mechanical Cycling," *Composites, Proceedings of the 8th International Conference on Composite Materials (ICCM8)*, Honolulu, HI, July 15–19. Section 12-21 (A92-32535 13-39). Covina, CA: Society for the Advancement of Material and Process Engineering, pp. 20-B-1 to 20-B-9.
20. M.G. Castelli, J.R. Ellis, and P.A. Bartolotta. 1990. "Thermomechanical Testing Techniques for High-Temperature Composites: TMF Behavior of SiC (SCS-6)/Ti-15-3," *NASA Technical Memorandum 103171*.
21. A.K. Noor and S.L. Venneri, senior editors. 1994. "New and Projected Aeronautical and Space Systems, Design Concepts and Loads," *Flight-Vehicle Materials, Structures, and Dynamics—Assessment and Future Directions.* New York: The American Society of Mechanical Engineers, Vol. 1, pp. 15–84.
22. Sir G. Sutton. 1965. *Mastery of the Air.* New York: Basic Books, Inc., pp. 157–166.
23. N.F. Harpur. 1967. "Concorde Structural Development," *AIAA Commercial Aircraft Design and Operation Meeting.* New York: American Institute of Aeronautics and Astronautics, pp. 1–14.
24. I.M. Daniel and O. Ishai. 1994. *Engineering Mechanics of Composite Materials.* New York: Oxford University Press, pp. 34–47.
25. B.Z. Jang. 1994. *Advanced Polymer Composites.* Materials Park, OH: ASM International, p. 93.
26. W.H. Prosser. 1991. "The Propagation of Characteristics of the Plate Modes of Acoustic Emission Waves in Thin Aluminum Plates and Thin Graphite/Epoxy Composite Plates and Tubes," *NASA Technical Memorandum* 104187.

On the Linear Viscoelasticity of Thin-Walled Laminated Composite Beams

PIZHONG QIAO*
Department of Civil Engineering
The University of Akron
Akron, OH 44325-3905

EVER J. BARBERO
Department of Mechanical and Aerospace Engineering
West Virginia University
Morgantown, WV 26506-6106

JULIO F. DAVALOS
Department of Civil and Environmental Engineering
West Virginia University
Morgantown, WV 26506-6103

(Received June 21, 1998)
(Revised May 28, 1999)

ABSTRACT: An analytical model to predict the linear viscoelastic behavior of thin-walled laminated fiber-reinforced plastic (FRP) composite beams is presented. Using the correspondence principle, this new model integrates micro/macro-mechanics of composites and mechanics of thin-walled laminated beams to perform beam analyses in the Laplace or Carson domains. The analytical expressions for beam relaxation coefficients are obtained. Using a collocation method, the flexural creep behavior of beams in the time domain is numerically solved. Predictions by the present model are compared favorably with experimental data for glass fiber-reinforced plastic structural laminates under tension and a box-beam under bending. The influence of beam fiber architecture and fiber volume fraction on the linear viscoelastic response for a wide-flange beam is examined to show that this model can be efficiently used in the flexural creep analysis and design of FRP structural shapes.

*Author to whom correspondence should be addressed.

0021-9983/00/01 0039–30 $10.00/0

INTRODUCTION

CREEP INDUCED DEFORMATION or damage of engineering structures may eventually lead to excessive deflections and catastrophic failure. Therefore, it is critical to predict the long-term response of a structure during its lifetime service. Viscoelasticity is an important concept for determining long-term behavior (service-life time) of structures. Viscoelasticity permits us to describe the behavior of materials exhibiting strain rate effects under applied loads. These effects are illustrated by creep phenomena under certain loads or by stress relaxation under a constant deformation. For most composites, the viscoelastic behavior is primarily due to the matrix. Composite materials are reinforced with fibers in part to resist creep deformation. The magnitude of the creep deformation induced in a composite structure under a certain loading is influenced by a variety of factors, such as material architecture, temperature, humidity, loading frequency, and stress level. Due to the variety of composite materials, it may be costly and difficult to characterize the creep behavior of composites through experimental tests. Also, the real time experimental tests under different temperature and moisture conditions are very time consuming and difficult to carry out. Therefore, a need exists to develop an analytical model which can accurately predict the creep behavior of composite structures and to verify this model with experimental data. The worldwide applications of cost effective pultruded glass fiber-reinforced composites in civil construction provide a motivation for the development of analytical models to characterize the long-term creep behavior of structural components made of composite materials.

In practical engineering design, deflections and stresses are very important criteria in reliability and serviceability evaluations of structures. The potential long-term viscoelastic, or creep behavior, response under loading must be anticipated and accommodated in design, because creep can lead to a gradual decrease of the structural effective stiffness and result in unacceptably large deformations. These effects may take place during a long time and may induce failures due to creep rupture. Therefore, the viscoelastic behavior of a composite structure over its life-span must be considered in design practice. Since most engineering structures are designed within the linear elastic range of the material and likely to function within a relatively narrow range of stresses, the material can be assumed to be linearly viscoelastic [1].

There is limited information available on flexural creep of composite structures. Lee and Ueng [2] proposed a "law of mixture" model for the creep behavior of a unidirectional composite to study the creep phenomenon of simple composite structures, such as a 3-bar truss and beam bending problems. However, the model predictions were not compared with any experimental data. Holmes and Rahman [3] conducted an experimental investigation on the creep behavior of glass reinforced plastic box-beams. The rate of tensile, compressive, and shear creep strains

as well as deflections were measured. However, no theoretical predictions related to their experimental data and materials exist.

Several mathematical models have been developed to predict the viscoelastic behavior of materials. These mechanistic models are essentially composed of springs and dashpots to simulate the elastic and viscous responses of materials (e.g., Maxwell and Maxwell-Voigt Models), where the spring and dashpot represent the initial elastic response and the time dependence property of the material, respectively [4]. The viscoelastic behavior of matrix and fiber can be represented by these models. Numerous micromechanics models are available to evaluate the viscoelastic properties of composites and can be used to predict the macromechanics properties of components. Hashin [5,6] first used the cylinder assemblage model to evaluate the macroscopic viscoelastic properties of fiber-reinforced materials. In the composite cylinder model, the correspondence principle is applied between the elastic and viscoelastic relaxation moduli of composites with identical phase geometry. Christensen [7] applied the same analogy with the composite sphere model to predict the effective modulus of composite materials. Laws and McLaughlin [8] estimated the viscoelastic creep compliance of composites by applying the self-consistent method. Wang and Weng [9] adopted the Eshelby-Mori-Tanaka method to obtain the overall linear viscoelastic properties of composites with different geometries of inclusions. The above studies indicated that many well developed micromechanical models for the elastic case could be extended to the viscoelastic range of composites and could efficiently predict the macroscopic behavior of the materials over time.

A model for linear viscoelastic solids with periodic microstructure was presented by Barbero and Luciano [10] and Luciano and Barbero [11]. They extended models for elastic solids with periodic microstructure [12,13] to the viscoelastic case and developed analytical expressions for the relaxation moduli of linear viscoelastic composites with periodic microstructure [11]. They derived closed-form expressions in the Laplace domain for the coefficient of the linear relaxation tensor of composite material with periodically distributed elastic inclusions (fibers) in the linear viscoelastic matrix. Assuming that the viscoelastic behavior of the matrix can be represented by a four-parameter (Maxwell-Voigt) model, the inversion of the linear relaxation tensors to the time domain was carried out analytically for composites reinforced with long fibers. Their micromechanics model can predict the creep response of fiber-reinforced composites with transverse isotropy without the use of empirical correction factors. Any geometry of fibers and spatial distribution of inclusions can be modeled, and it can be further applied to predict the long term viscoelastic behavior of fiber-reinforced plastic (FRP) composite structures. Harris [14] and Harris and Barbero [1] combined this model with a macromechanics model to predict the viscoelastic behaviors of composite laminates under tensile loads, and a good correlation with experiments under various environmental effects was obtained. It is envisaged that this micro/macromechanics model can be combined with a structural model to predict the linear viscoelastic behavior of composite structures at the component level (e.g., beams and columns).

Several structural models are available to evaluate the linear elastic behaviors of laminated composite beams under bending [15] and torsion [16,17]. The approach proposed by Whitney et al. [18] and Tsai [19] considered that the effective moduli of a laminated beam are computed from the reciprocals of the components of the corresponding laminate compliance matrix, which is obtained by full inversion of the laminate stiffness matrix. The basic assumption in this approach is that the resultant force and moment generated by the transverse normal stresses are negligible. This approach was adopted by Barbero et al. [15] to model thin-walled laminated composite beams with open or closed-sections using first-order shear deformation theory. In the Mechanics of Laminated Beams (MLB) [15], the bending response of FRP beams is evaluated by considering that the stiffness coefficients of a beam are computed by adding the contributions of the stiffnesses of the component panel laminates, which in turn are obtained from the effective moduli of laminates. This model accounts for membrane (in-plane) and flexure stiffnesses of the thin-walled panels, and the beam deflections are obtained from Timoshenko's beam solution, which contains both bending and shear deflections. Davalos et al. [20] showed that an experimentally-verified micro/macromechanics model combined with MLB can accurately predict the linear elastic beam response of FRP structural shapes in bending. In this combined micro/macromechanics model, the ply stiffnesses and panel laminate properties are predicted by micromechanics formulas [13] and macromechanics, and the overall response of FRP beams in bending is analyzed by MLB. However, no theory has been developed for linear viscoelastic behavior of FRP structural shapes. The successful application of micro/macromechanics models with MLB in the elastic domain provides motivation for developing a model for the viscoelastic response of laminated composite beams.

Therefore, the objective of this study is to extend the model of linear viscoelastic composites with periodic microstructure to predict the creep responses of thin-walled laminated FRP beams. Based on the Mechanics of Laminated composite Beams (MLB) [15,20], the analytical expressions for beam relaxation coefficients in Carson domain are developed, and the long term bending responses of laminated beams are derived. The inversion to the time domain is solved numerically by a collocation method [21] and the creep behavior of beams is analyzed. In addition, a systematic computer code to predict behaviors of laminated FRP composite beams is developed. A pultruded FRP box-beam is experimentally tested under sustained loading to validate the proposed model. Finally, the influence of material architecture, such as fiber orientation and fiber volume fraction, on the creep flexural responses of FRP beams is discussed.

VISCOELASTICITY OF LAMINATED COMPOSITE BEAMS

The viscoelastic problem of composite materials with periodic microstructure has been presented by Luciano and Barbero [11]. The assumptions used are that the matrix is linear viscoelastic and the fibers are elastic. The viscoelastic Correspondence Principle is applied and the problem is solved in the Carson domain, where the formulas for the relaxation functions of transversely isotropic composites are expressed in terms of the properties of the matrix and the fibers and account for the geometry of the inclusions. The ply relaxation matrices in the Carson domain can then be obtained in terms of the relaxation tensors by using plane stress assumptions. In the Carson domain, the laminate relaxation matrix $(\hat{A}, \hat{B}, \hat{D})$ can be derived using Classical Lamination Theory (CLT), and the beam relaxation coefficients can be further obtained based on the Mechanics of Laminated composite Beams (MLB); the formulas for the beam linear viscoelastic behavior under bending can be derived in the Carson domain, as shown in the following sections.

Viscoelastic Constitutive Equations and Material Properties

If there is no stress or strain existing before time $t = 0$, the constitutive equation for viscoelastic material [21] can be expressed in the time domain as:

$$\epsilon(t) = \int_0^t J(t-\tau)\frac{\partial\sigma}{\partial\tau}d\tau$$

$$\sigma(t) = \int_0^t E(t-\tau)\frac{\partial\epsilon}{\partial\tau}d\tau \tag{1}$$

where $J(t)$ and $E(t)$ are the 1-D creep compliance and relaxation tensors, respectively. Using the Correspondence Principle, a relationship between the relaxation tensor and the creep compliance tensor can be found. The Carson transform [8] of a function $f(t)$ is denoted as

$$\hat{f}(s) = s\int_0^\infty e^{-st} f(t)dt \tag{2}$$

then Equation (1) can be expressed in the Carson domain as

$$\hat{\epsilon}(s) = \hat{M}(s)\hat{\sigma}(s)$$

$$\hat{\sigma}(s) = \hat{L}(s)\hat{\epsilon}(s) \tag{3}$$

where the Carson transform of the creep compliance $\hat{M}(s)$ and the relaxation tensor $\hat{L}(s)$ satisfies the following relation:

$$\hat{L}(s)\hat{M}(s) = \hat{M}(s)\hat{L}(s) = I \quad (4)$$

which is the usual formula for the calculation of $\hat{L}(s)$ when $\hat{M}(s)$ is given or vice versa [8].

Since most conventional fibers used today in composite materials display little or no creep effects, the fibers can be assumed to behave elastically. Hence, the viscoelastic compliance moduli of composites depend mainly on the viscoelastic response of the matrix. In this study, the matrix is assumed as linear viscoelastic and the fibers as elastic. By using this assumption, we can obtain the compliance moduli of composites using micromechanics formulas [11,22]. The viscoelastic properties (creep compliance) of matrix in the secondary creep (steady-state) range are approximated by the Maxwell model [4] as

$$M(t) = \frac{1}{E^M} + \frac{t}{\mu^M} \quad (5)$$

where $1/E^M$ is the initial modified compliance modulus of matrix; E^M is the elastic modulus E^e plus the effect of all primary creep deformations lumped at time $t = 0$; μ^M is the inverse of the slope of the secondary compliance creep. Both values are obtained from the creep testing of the matrix only. E^M is not the true initial elastic modulus of the material, because the Maxwell model neglects the primary creep region which typically occurs over a short time compared to the secondary creep response of the material. Since the modeling of the primary creep that occurs over a short period is often negligible in structural design, and the main interest is on the response for a long period of time, the Maxwell model provides a good representation over long-time ranges for both neat matrix and composites [1] and is used in this study. The expression of Equation (5) in the Carson domain becomes

$$\hat{M}(s) = \frac{1}{E^M} + \frac{1}{s\mu^M} \quad (6)$$

From Equation (4), the effective relaxation modulus $\hat{E}_0$ of matrix, which is the inverse of creep compliance [Equation (6)], is expressed as

$$\hat{E}_0 = \hat{L}(s) = \frac{1}{\hat{M}(s)} = \frac{sE^M\mu^M}{E^M + s\mu^M} \quad (7)$$

and the Lamé properties of matrix are expressed in terms of $\hat{E}_0$ as

$$\hat{\lambda}_0 = \frac{\hat{E}_0\nu_0}{(1+\nu_0)(1-2\nu_0)} \qquad \mu_0 = \frac{\hat{E}_0}{2(1+\nu_0)} \quad (8)$$

Since the fibers remain elastic, the Lamé properties of fibers in terms of the fiber modulus E_1 are

$$\lambda_1 = \frac{E_1\nu_1}{(1+\nu_1)(1-2\nu_1)} \qquad \mu_1 = \frac{E_1}{2(1+\nu_1)} \quad (9)$$

Consistent with the literature [9,21], the Poisson ratios of matrix (ν_0) and fibers (ν_1) are assumed to remain constants in time.

Micro/Macromechanics of Composites in the Carson Domain

In this section, the analytical expression of relaxation tensors for unidirectional composite with periodic microstructure are first introduced. Then, transversely isotropic relaxation tensors in the Carson domain are obtained by an averaging procedure. An FRP laminate or panel that is manufactured by the pultrusion process can be simulated as a layered system, and the panel's relaxation moduli in the Carson domain can be computed by Classical Lamination Theory (CLT) in terms of the ply relaxation tensors.

UNIDIRECTIONAL COMPOSITES WITH PERIODIC MICROSTRUCTURE

Using Fourier series techniques to describe materials with periodically distributed voids or inclusions, the mechanical behavior of composite materials with periodic microstructure was first introduced by Nemat-Nasser and Taya [23]. A general procedure to analytically evaluate the overall properties of composites with periodic elastic inclusions or voids was developed by Iwakuma and Nemat-Nasser [12]. This procedure can be extended to estimate the overall elastic moduli of composite materials but it entails considerable numerical effort. Luciano and Barbero [13] presented closed-form expressions for the coefficients of the stiffness tensor and the elastic moduli of unidirectional composite materials with periodically and randomly distributed fibers. Applying similar analytical expressions in the Laplace domain, they obtained the overall linear viscoelastic relaxation tensors for composites with periodic inclusions [11].

For unidirectional composites reinforced by long circular cylindrical fibers along the x_1 axis, the linear viscoelastic relaxation tensors $(\hat{L}^*)$ in the Carson domain are expressed as (the expressions in the Laplace domain are given by Luciano and Barbero [11])

$$\hat{L}^*_{11}(s) = \hat{\lambda}_0 + 2\hat{\mu}_0 - V_f\left[\frac{S_3^2}{\hat{\mu}_0^2} - \frac{2S_6S_3}{\hat{\mu}_0^2 g} - \frac{aS_3}{\hat{\mu}_0 c} + \frac{S_6^2 - S_7^2}{\hat{\mu}_0^2 g^2} + \frac{aS_6 + bS_7}{\hat{\mu}_0 gc} + \frac{a^2 - b^2}{4c^2}\right]/H$$

$$\hat{L}^*_{12}(s) = \hat{\lambda}_0 + V_f b\left[\frac{S_3}{2c\hat{\mu}_0} - 2\frac{S_6 - S_7}{2c\hat{\mu}_0 g} - \frac{a+b}{4c^2}\right]/H$$

$$\hat{L}^*_{23}(s) = \hat{\lambda}_0 + V_f\left[\frac{aS_7}{2\hat{\mu}_0 gc} - \frac{ba + b^2}{4c^2}\right]/H \tag{10}$$

$$\hat{L}^*_{22}(s) = \hat{\lambda}_0 + 2\hat{\mu}_0 - V_f\left[-\frac{aS_3}{2\hat{\mu}_0 c} + \frac{aS_6}{2\hat{\mu}_0 gc} + \frac{a^2 - b^2}{4c^2}\right]/H$$

$$\hat{L}^*_{44}(s) = \hat{\mu}_0 - V_f\left[-\frac{2S_3}{\hat{\mu}_0} + (\hat{\mu}_0 - \mu_1)^{-1} + \frac{4S_7}{\hat{\mu}_0(2 - 2\nu_0)}\right]^{-1}$$

$$L^*_{66}(s) = \hat{\mu}_0 - V_f\left[-\frac{S_3}{\hat{\mu}_0} + (\hat{\mu}_0 - \mu_1)^{-1}\right]^{-1}$$

where V_f is the fiber volume fraction, and the coefficients of a, b, c, g and H are given by

$$a = \mu_1 - \hat{\mu}_0 - 2\mu_1\nu_0 + 2\hat{\mu}_0\nu_1$$

$$b = \nu_1\mu_1 - \hat{\mu}_0\nu_0 - 2\mu_1\nu_0\nu_1 + 2\hat{\mu}_1\nu_0\nu_1$$

$$c = (\hat{\mu}_0 - \mu_1)(\mu_1 - \hat{\mu}_0 - 2\mu_1\nu_0 - \hat{\mu}_0\nu_0 + \mu_1\nu_1 + 2\hat{\mu}_0\nu_1 + \mu_1\nu_1 + 2\hat{\mu}_0\nu_0\nu_1 - 2\mu_1\nu_0\nu_1)$$

$$g = 2 - 2\nu_0$$

and

$$H = \frac{aS_3^2}{2\hat{\mu}_0^2 c} - \frac{aS_6S_3}{\hat{\mu}_0^2 gc} + \frac{a(S_6^2 - S_7^2)}{2\hat{\mu}_0^2 g^2 c} + \frac{S_3(b^2 - a^2)}{2\hat{\mu}_0 c^2} + \frac{S_6(a^2 - b^2) + S_7(ab + b^2)}{2\hat{\mu}_0 gc^2} + \frac{a^3 - 2b^3 - 3ab^2}{8c^3}$$

The series S_3, S_6, and S_7 are obtained from Nemat-Nasser et al. [23] accounting for the geometries of the fibers and are expressed as parabolic functions [13]:

$$S_3 = 0.49247 - 0.47603V_f - 0.02748V_f^2$$

$$S_6 = 0.36844 - 0.14944V_f - 0.27152V_f^2 \tag{11}$$

$$S_7 = 0.12346 - 0.32035V_f + 0.23517V_f^2$$

VISCOELASTIC PROPERTIES OF TRANSVERSELY ISOTROPIC MATERIAL

Due to the periodicity of the microstructure, the linear viscoelastic relaxation tensors for unidirectional composite represent an orthotropic material with square symmetry. To model composites with transverse isotropy, the following averaging procedure [21] is used to obtain the relaxation tensor $\hat{C}^*$ of the transversely isotropic material

$$\hat{C}^* = \frac{1}{\pi}\int_0^{\pi}[T(\theta)]\hat{L}^*[T(\theta)]^T\,d\theta \tag{12}$$

where θ is the rotation about the x_1 axis of the $\hat{L}^*$ tensor and $T(\theta)$ is the fourth-order orthogonal rotation tensor. After the integration of Equation (12), the relaxation tensors of transversely isotropic material $(\hat{C}^*)$ are expressed explicitly in terms of the relaxation tensors $(\hat{L}^*)$ of unidirectional composites as

$$\hat{C}^*_{11}(s) = \hat{L}^*_{11}(s)$$

$$\hat{C}^*_{12}(s) = \hat{L}^*_{12}(s)$$

$$\hat{C}^*_{22}(s) = \frac{3}{4}\hat{L}^*_{22}(s) + \frac{1}{4}\hat{L}^*_{23}(s) + \frac{1}{2}\hat{L}^*_{44}(s) \tag{13}$$

$$\hat{C}^*_{23}(s) = \frac{1}{4}\hat{L}^*_{22}(s) + \frac{3}{4}\hat{L}^*_{23}(s) - \frac{1}{2}\hat{L}^*_{44}(s)$$

$$\hat{C}^*_{66}(s) = \hat{L}^*_{66}(s)$$

$$\hat{C}^*_{44}(s) = \frac{1}{2}\hat{C}^*_{22}(s) - \frac{1}{2}\hat{C}^*_{23}(s) = \frac{1}{4}\hat{L}^*_{22}(s) - \frac{1}{4}\hat{L}^*_{22}(s) + \frac{1}{2}\hat{L}^*_{44}(s)$$

The constitutive equation (Hooke's law) for a transversely isotropic material [21], with the axis of symmetry along x_1, is then expressed as

$$\begin{Bmatrix} \hat{\sigma}_{11} \\ \hat{\sigma}_{22} \\ \hat{\sigma}_{33} \\ \hat{\sigma}_{23} \\ \hat{\sigma}_{13} \\ \hat{\sigma}_{12} \end{Bmatrix} = \begin{bmatrix} \hat{C}^*_{11} & \hat{C}^*_{12} & \hat{C}^*_{12} & 0 & 0 & 0 \\ \hat{C}^*_{12} & \hat{C}^*_{22} & \hat{C}^*_{23} & 0 & 0 & 0 \\ \hat{C}^*_{12} & \hat{C}^*_{23} & \hat{C}^*_{22} & 0 & 0 & 0 \\ 0 & 0 & 0 & \hat{C}^*_{44} & 0 & 0 \\ 0 & 0 & 0 & 0 & \hat{C}^*_{66} & 0 \\ 0 & 0 & 0 & 0 & 0 & \hat{C}^*_{66} \end{bmatrix} \begin{Bmatrix} \hat{\epsilon}_{11} \\ \hat{\epsilon}_{22} \\ \hat{\epsilon}_{33} \\ \hat{\gamma}_{23} \\ \hat{\gamma}_{13} \\ \hat{\gamma}_{12} \end{Bmatrix} \tag{14}$$

To model a ply, the assumption of plane stress is used, and the constitutive relationship for a unidirectional composite reduces to

$$\begin{Bmatrix} \hat{\sigma}_{11} \\ \hat{\sigma}_{22} \\ \hat{\sigma}_{12} \end{Bmatrix} = \begin{bmatrix} \hat{Q}^*_{11} & \hat{Q}^*_{12} & 0 \\ \hat{Q}^*_{12} & \hat{Q}^*_{22} & 0 \\ 0 & 0 & \hat{Q}^*_{66} \end{bmatrix} \begin{Bmatrix} \hat{\epsilon}_{11} \\ \hat{\epsilon}_{22} \\ \hat{\gamma}_{11} \end{Bmatrix} \tag{15}$$

where the reduced relaxation coefficients $\hat{Q}^*$ are given by

$$\begin{aligned} \hat{Q}^*_{11} &= \hat{C}^*_{11} - \frac{\hat{C}^{*2}_{12}}{\hat{C}^*_{22}} \\ \hat{Q}^*_{12} = \hat{Q}^*_{21} &= \hat{C}^*_{12} - \frac{\hat{C}^*_{23}\hat{C}^*_{12}}{\hat{C}^*_{22}} \\ \hat{Q}^*_{22} &= \hat{C}^*_{22} - \frac{\hat{C}^{*2}_{23}}{\hat{C}^*_{22}} \\ \hat{Q}^*_{66} &= \hat{C}^*_{66} \end{aligned} \tag{16}$$

For a typical pultruded FRP section, each laminate or panel can be simulated as a laminated configuration and mainly includes the following three types of layers [20]: (1) Continuous Strand Mats (CSM); (2) angle- or cross-ply Stitched Fabrics (SF); and (3) rovings or unidirectional fiber bundles. The SF and roving layers are usually modeled as unidirectional composites with distinct orientations, and their

reduced relaxation coefficients $\hat{Q}^*$ are obtained from Equation (16); their transformed reduced relaxation coefficients are obtained through appropriate transformation matrices. The CSM layer is assumed to be isotropic in the plane, and the properties can be obtained from approximate relations [24]. A new model for determining the properties and reduced relaxation coefficients for a CSM layer was presented by Harris and Barbero [1]; adopting the averaging procedure in the plane as

$$(\hat{Q}^*)_{CSM} = \frac{1}{\pi}\int_0^{\pi} [B(\theta)][\hat{Q}^*][B(\theta)]^T \, d\theta \tag{17}$$

where $[B(\theta)]$ is the transformation matrix for in-plane rotation and is given by

$$[B(\theta)] = \begin{bmatrix} \cos^2\theta & \sin^2\theta & -\sin\theta\cos\theta \\ \sin^2\theta & \cos^2\theta & 2\sin\theta\cos\theta \\ \sin\theta\cos\theta & -\sin\theta\cos\theta & \cos^2\theta - \sin^2\theta \end{bmatrix} \tag{18}$$

After completing the integral, the following reduced relaxation coefficients for a CSM layer are given explicitly as

$$\begin{aligned} (\hat{Q}^*_{11})_{CSM} &= \frac{3}{8}\hat{Q}^*_{11} + \frac{1}{4}\hat{Q}^*_{12} + \frac{3}{8}\hat{Q}^*_{22} + \frac{1}{2}\hat{Q}^*_{66} \\ (\hat{Q}^*_{12})_{CSM} = (\hat{Q}^*_{21})_{CSM} &= \frac{1}{8}\hat{Q}^*_{11} + \frac{3}{4}\hat{Q}^*_{12} + \frac{1}{8}\hat{Q}^*_{22} - \frac{1}{2}\hat{Q}^*_{66} \\ (\hat{Q}^*_{22})_{CSM} &= \frac{3}{8}\hat{Q}^*_{11} + \frac{1}{4}\hat{Q}^*_{12} + \frac{3}{8}\hat{Q}^*_{22} + \frac{1}{2}\hat{Q}^*_{66} \\ (\hat{Q}^*_{66})_{CSM} &= \frac{1}{8}\hat{Q}^*_{11} - \frac{1}{4}\hat{Q}^*_{12} + \frac{1}{8}\hat{Q}^*_{22} + \frac{1}{2}\hat{Q}^*_{66} \end{aligned} \tag{19}$$

with all other coefficients being equal to zero.

LAMINATE RELAXATION COEFFICIENTS

Once the reduced relaxation coefficients of corresponding layers are computed, the relaxation matrices of an ith panel ($[\hat{A}]_i$, $[\hat{B}]_i$, $[\hat{D}]_i$) in the Carson domain can be computed from Classical Lamination Theory (CLT). In particular, the panel creep compliance matrix, which is obtained by inversion of the extensional relaxation matrix $[\hat{A}]_i$, is used to compute the creep compliance coefficients and relaxation moduli of the ith panel $(\hat{E}_x, \hat{E}_y, \hat{G}_{xy})$, as shown in the work by Harris and Barbero [1].

Mechanics of Thin-Walled Lamination Beams in the Carson Domain

A formal engineering approach to the mechanics of thin-walled laminated beams (MLB) [15], based on kinematic assumptions consistent with Timoshenko beam theory, is incorporated in this study to model the overall viscoelastic response of pultruded FRP sections.

BASIC ASSUMPTIONS AND COORDINATE SYSTEMS

Straight FRP beams with at least one axis of geometric and material symmetry are considered. The FRP sections are modeled as assemblies of flat panels. We define a global coordinate system (X, Y, Z), with the Z-axis parallel to the axis of the beam, and a local coordinate system (x_i, y_i, z_i) for each panel, with the z-axis perpendicular to the plane of the panel and the x_i-axis as the longitudinal direction of panel (Figure 1). Based on Timoshenko beam theory, two basic assumptions are used in MLB. First, the beam contour does not deform in its own plane, and therefore, the in-plane (beam cross-section) motions are functions of the beam axis only. The second assumption is that a plane section originally normal to the beam axis remains plane, but not necessarily normal to the beam axis due to shear deformation.

BEAM RELAXATION COEFFICIENTS

For a laminated panel, the general constitutive relation between resultant forces and moments and midsurface strains and curvatures is given by CLT as

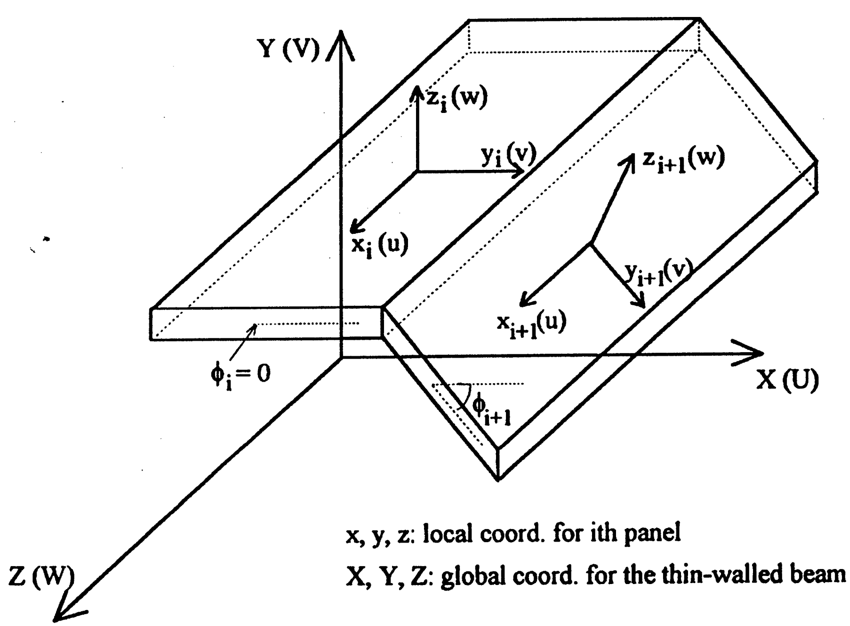

Figure 1. *Global (beam) and local (panel) coordinator systems.*

$$\begin{Bmatrix} \hat{N}_x \\ \hat{N}_y \\ \hat{N}_{xy} \\ \hat{M}_x \\ \hat{M}_y \\ \hat{M}_{xy} \end{Bmatrix} = \begin{bmatrix} \hat{A}_{11} & \hat{A}_{12} & \hat{A}_{16} & \hat{B}_{11} & \hat{B}_{12} & \hat{B}_{16} \\ \hat{A}_{12} & \hat{A}_{22} & \hat{A}_{26} & \hat{B}_{12} & \hat{B}_{22} & \hat{B}_{26} \\ \hat{A}_{16} & \hat{A}_{26} & \hat{A}_{66} & \hat{B}_{16} & \hat{B}_{26} & \hat{B}_{66} \\ \hat{B}_{11} & \hat{B}_{12} & \hat{B}_{16} & \hat{D}_{11} & \hat{D}_{12} & \hat{D}_{16} \\ \hat{B}_{12} & \hat{B}_{22} & \hat{B}_{26} & \hat{D}_{12} & \hat{D}_{22} & \hat{D}_{26} \\ \hat{B}_{16} & \hat{B}_{26} & \hat{B}_{66} & \hat{D}_{16} & \hat{D}_{26} & \hat{D}_{66} \end{bmatrix} \begin{Bmatrix} \hat{\epsilon}_x^0 \\ \hat{\epsilon}_y^0 \\ \hat{\epsilon}_{xy}^0 \\ \hat{\kappa}_x^0 \\ \hat{\kappa}_y^0 \\ \hat{\kappa}_{xy}^0 \end{Bmatrix} \tag{20}$$

where $[\hat{A}]_i$, $[\hat{B}]_i$, and $[\hat{D}]_i$ are the ith panel relaxation submatrices in the Carson domain as introduced in laminate relaxation coefficients. By full inversion of the panel relaxation matrix [Equation (20)], we can express the midsurface strains $(\hat{\epsilon}_x^0, \hat{\epsilon}_y^0, \hat{\gamma}_{xy}^0)$ and curvatures $(\hat{\kappa}_x, \hat{\kappa}_y, \hat{\kappa}_{xy})$ in terms of the creep compliance coefficients and panel resultant forces as:

$$\begin{Bmatrix} \hat{\epsilon}_x^0 \\ \hat{\epsilon}_y^0 \\ \hat{\gamma}_{xy}^0 \\ \hat{\kappa}_x \\ \hat{\kappa}_y \\ \hat{\kappa}_{xy} \end{Bmatrix} = \begin{bmatrix} \hat{\alpha}_{11} & \hat{\alpha}_{12} & \hat{\alpha}_{16} & \hat{\beta}_{11} & \hat{\beta}_{12} & \hat{\beta}_{16} \\ \hat{\alpha}_{12} & \hat{\alpha}_{22} & \hat{\alpha}_{26} & \hat{\beta}_{12} & \hat{\beta}_{22} & \hat{\beta}_{26} \\ \hat{\alpha}_{16} & \hat{\alpha}_{26} & \hat{\alpha}_{66} & \hat{\beta}_{16} & \hat{\beta}_{26} & \hat{\beta}_{16} \\ \hat{\beta}_{11} & \hat{\beta}_{12} & \hat{\beta}_{16} & \hat{\delta}_{11} & \hat{\delta}_{12} & \hat{\delta}_{16} \\ \hat{\beta}_{12} & \hat{\beta}_{22} & \hat{\beta}_{26} & \hat{\delta}_{12} & \hat{\delta}_{22} & \hat{\delta}_{26} \\ \hat{\beta}_{16} & \hat{\beta}_{26} & \hat{\beta}_{66} & \hat{\delta}_{16} & \hat{\delta}_{26} & \hat{\delta}_{66} \end{bmatrix} \begin{Bmatrix} \hat{N}_x \\ \hat{N}_y \\ \hat{N}_{xy} \\ \hat{M}_x \\ \hat{M}_y \\ \hat{M}_{xy} \end{Bmatrix} \tag{21}$$

where $[\hat{\alpha}]_i$, $[\hat{\beta}]_i$ and $[\hat{\delta}]_i$ are the panel creep compliance submatrices in the Carson domain. Consistent with beam theory and based on the above given assumptions, we consider for each panel (Figure 1) that the resultant force and moment generated by the transverse normal stresses (in the y_i direction) are negligible:

$$\hat{N}_y = \hat{M}_y = 0 \tag{22}$$

For bending without torsion, we can further state that

$$\hat{M}_{xy} = 0 \tag{23}$$

Considering Equations (22) and (23), Equation (21) reduces to

$$\begin{Bmatrix} \hat{\hat{\epsilon}}_x \\ \hat{\hat{\kappa}}_x \\ \hat{\hat{\gamma}}_{xy} \end{Bmatrix} = \begin{bmatrix} \hat{\alpha}_{11} & \hat{\beta}_{11} & \hat{\alpha}_{16} \\ \hat{\beta}_{11} & \hat{\delta}_{11} & \hat{\beta}_{16} \\ \hat{\alpha}_{16} & \hat{\beta}_{16} & \hat{\alpha}_{66} \end{bmatrix} \begin{Bmatrix} \hat{\hat{N}}_x \\ \hat{\hat{M}}_x \\ \hat{\hat{N}}_{xy} \end{Bmatrix} \tag{24}$$

where the overbar identifies a panel quantity. By restricting the off-axis plies to be balanced symmetric (for most pultruded FRP sections, the off-axis plies are manufactured with balanced symmetric patterns), the shear-extension ($\hat{\alpha}_{16}$) and shear-bending ($\hat{\beta}_{16}$) coupling creep compliance coefficients in Equation (24) vanish:

$$\hat{\alpha}_{16} = \hat{\beta}_{16} = 0 \tag{25}$$

Then, by inverting the creep compliance matrix in Equation (24), we can obtain the relaxation matrix of the ith panel of a thin-walled laminated beam as:

$$\begin{Bmatrix} \hat{\bar{N}}_x \\ \hat{\bar{M}}_x \\ \hat{\bar{N}}_{xy} \end{Bmatrix} = \begin{bmatrix} \hat{\bar{A}}_i & \hat{\bar{B}}_i & 0 \\ \hat{\bar{B}}_i & \hat{\bar{D}}_i & 0 \\ 0 & 0 & \hat{\bar{F}}_i \end{bmatrix} \begin{Bmatrix} \hat{\bar{\epsilon}}_x \\ \hat{\bar{\kappa}}_x \\ \hat{\bar{\gamma}}_x \end{Bmatrix} \tag{26}$$

where $\hat{\bar{A}}_i, \hat{\bar{B}}_i, \hat{\bar{D}}_i$, and $\hat{\bar{F}}_i$ are, respectively, the ith panel extensional, bending-extensions, bending, and shear relaxation coefficients in the Carson domain.

General expression for the beam relaxation coefficients are derived from the beam variational formulation [15]. Hence, beam axial ($\hat{A}_Z$), bending-extension coupling ($\hat{B}_Y$), bending $\hat{D}_Y$), and shear ($\hat{F}_Y$) relaxation coefficients that account for the contribution of all the panels can be computed as:

$$\hat{A}_Z = \sum_{i=1}^{n} \hat{\bar{A}}_i b_i$$

$$\hat{B}_Y = \sum_{i=1}^{n} [\hat{\bar{A}}_i(\bar{Y}_i - Y_n) + \hat{\bar{B}}_i \cos\phi_i] b_i$$

$$\hat{D}_Y = \sum_{i=1}^{n} \left[\hat{\bar{A}}_i \left((\bar{Y}_i - Y_n)^2 + \frac{b_i}{12} \sin^2\phi_i \right) + 2\hat{\bar{B}}_i(\bar{Y}_i - Y_n)\cos\phi_i + \hat{\bar{D}}_i \cos^2\phi_i \right] b_i \tag{27}$$

$$\hat{F}_Y = \sum_{i=1}^{n} \hat{\bar{F}}_i b_i \sin^2\phi_i$$

By imposing the condition $\hat{B}_Y = 0$, the neutral axis of bending is defined by the coordinate Y_n as

$$Y_n = \frac{\sum_{i=1}^{n} (\bar{Y}_i \hat{\bar{A}}_i + \cos\phi_i \hat{\bar{B}}_i) b_i}{\hat{A}_Z} \tag{28}$$

The shear correction factor $\hat{K}_Y$ in the Carson domain can be derived in a similar manner as for the elastic case [15]. As an approximation in design [20], the shear correction factor for pultruded sections can be taken as 1.0. In this study, we assume that the shear correction factor $\hat{K}_Y$ equals 1.0 for pultruded FRP sections and remains the same in both elastic and viscoelastic domains.

PREDICTION OF BEAM CREEP DEFLECTIONS AND STRAINS

Viscoelastic displacement and rotation function can be obtained by solving the Timoshenko beam equilibrium equations. Viscoelastic deflections at discrete locations can be computed by employing energy methods that incorporate the beam bending and shear relaxation coefficients. General formulas for maximum bending and shear deflections for typical beam loading and boundary conditions are available in manuals. For example, the creep central deflection for a three-point bending of a beam of span L and load P_Y applied at the center is:

$$\hat{\delta}_{Total} = \hat{\delta}_{Bending} + \hat{\delta}_{Shear} = \frac{P_Y L^3}{48\hat{D}_Y} + \frac{P_Y L}{4\hat{K}_Y \hat{F}_Y} \tag{29}$$

Thus, in the present formulation, the deflection components due to bending and shear can be separately evaluated.

For the ith panel, the midsurface viscoelastic strains and curvatures in terms of the beam resultant forces and moments are calculated as

$$\hat{\bar{\epsilon}}_y = \frac{N_Z}{\hat{A}_Z} + (\bar{Y}_i - Y_n)\frac{M_Y}{\hat{D}_Y}$$

$$\hat{\bar{\kappa}}_y = \frac{M_Y}{\hat{D}_Y} \cos\phi_i \tag{30}$$

$$\hat{\bar{\gamma}}_{xy} = \frac{V_Y}{\hat{K}_Y \hat{F}_Y} \sin\phi_i$$

where N_Z, M_Y, and V_Y are, respectively, the resultant internal axial force, bending moment, and shear force acting on the beam. Then, applying Equation (26), we can obtain the resultant forces and moments acting on the ith panel: $\hat{\bar{N}}_x, \hat{\bar{M}}_x$ and $\hat{\bar{N}}_{xy}$. Combining the constitutive relations of Equation (21) with the assumptions of Equations (22) and (23), the midsurface creep strains and curvatures on the ith panel are obtained as:

$$\begin{Bmatrix} \hat{\epsilon}_x^0 \\ \hat{\epsilon}_y^0 \\ \hat{\gamma}_{xy}^0 \\ \hat{\kappa}_x \\ \hat{\kappa}_y \\ \hat{\kappa}_{xy} \end{Bmatrix} = \begin{bmatrix} \hat{\alpha}_{11} & \hat{\alpha}_{16} & \hat{\beta}_{11} \\ \bar{\alpha}_{12} & \bar{\alpha}_{26} & \bar{\beta}_{12} \\ \bar{\alpha}_{16} & \bar{\alpha}_{66} & \bar{\beta}_{16} \\ \bar{\beta}_{11} & \bar{\beta}_{16} & \bar{\delta}_{11} \\ \bar{\beta}_{12} & \bar{\beta}_{26} & \bar{\delta}_{12} \\ \bar{\beta}_{16} & \bar{\beta}_{66} & \bar{\delta}_{16} \end{bmatrix} \begin{Bmatrix} \hat{N}_x \\ \hat{N}_{xy} \\ \hat{M}_x \end{Bmatrix} \tag{31}$$

where the overbar identifies a panel quantity. Based on classical lamination theory (CLT), we can obtain the ply creep strains through the thickness of each panel ($\hat{\epsilon}_x, \hat{\epsilon}_y$, and $\hat{\epsilon}_{xy}$) in the Carson domain. Using coordinate transformations, the ply creep strains ($\hat{\epsilon}_1, \hat{\epsilon}_2$, and $\hat{\gamma}_{12}$) in the Carson domain can also be computed in principal material directions.

NUMERICAL ANALYSIS OF COMPOSITE IN TIME DOMAIN

The equations for viscoelastic analysis of composite beams presented above are valid in the Carson domain. The inversion of these formulations from the Carson domain to the time domain can be carried out numerically by using a numerical collocation method [21], if the viscoelastic behavior of the matrix is known.

Collocation Method

The collocation method [21] performs the inverse Laplace of functions in the Laplace or Carson domain and obtains discrete values in time domain as

$$h(t) = Laplace^{-1}[\tilde{f}(s)] = Laplace^{-1}\left[\frac{\hat{f}(s)}{s}\right] \tag{32}$$

where $h(t)$ is the time domain function; $\tilde{f}(s)$ and $\hat{f}(s)$ are, respectively, the functions in the Laplace and Carson domains. This method uses the Legendre polynomials of order N to approximate the solution in the interval of $(-1,1)$; then the roots of polynomials are shifted and adjusted in the time scale. This numerical inversion technique provides N output data points ($N = 5$ is used in this study). An additional point can be obtained at $t = 0$ using the initial value theorem:

$$h(t=0) = \lim_{s \to \infty} \hat{f}(s) \tag{33}$$

Therefore, there are $N + 1$ known values available in the time domain, and they can be fitted by corresponding empirical models.

Fitting Models

In this study, we use both power-law and linear functions to fit the numerical data of viscoelastic responses in the time domain. A power-law is given as

$$h(t) = C_0 + C_n t^{\eta} \tag{34}$$

where for $t = 0$, we get $C_0 = h(0)$. The natural log of Equation (34) is expressed in compact form as

$$y = a + \eta x \tag{35}$$

where $y = \ln(h(t) - C_0)$ and $x = \ln(t)$. A linear regression technique is then used to obtain the parameters a and η. Since the secondary creep behavior of composites often shows a linear response with time, we could also use a linear function directly to fit the numerical data of viscoelastic response. In this study, the "multiple correlation coefficient," R^2, is used to evaluate the goodness-of-fit.

Computer Program: FRPCREEP

Based on the above viscoelastic theory for FRP beams and numerical models for the solution of the viscoelasticity of composites in time domain, the computer program FRPCREEP (flowchart shown in Figure 2) is developed to predict the

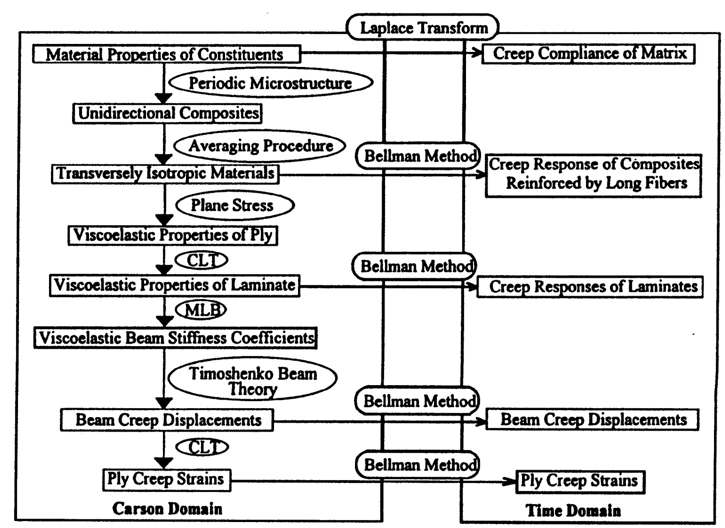

Figure 2. *Computational flowchart of FRPCREEP program.*

viscoelastic behavior of composite beams, from the viscoelastic constituent material properties to the creep flexural responses of thin-walled FRP beams. This program can predict the creep responses of FRP panels as well as thin-walled beams under tension or bending.

APPLICATIONS

Several studies on the applications of the above systematic approach are presented in this section. To validate the model, experimental data on viscoelastic responses of FRP laminates and beams are compared with the predicted values by the present theory. Parametric studies are also performed to study the influences of the fiber architecture and fiber volume fraction on creep behavior.

Viscoelastic Response of Laminates

Comparisons between experimental and analytical results for composite laminates under tension are presented, and a parametric study of laminate creep compliance coefficients as functions of fiber orientations is carried out.

GLASS-FRP LAMINATES UNDER TENSILE LOADS

Harris [14] measured the creep responses of neat vinylester matrix and several glass fiber-reinforced plastic (FRP) laminates under tension. The laminates were fabricated using glass fibers [$E_f = 72.5$ GPa (10.5×10^6 psi) and $\nu_f = 0.22$] and vinylester resins. The specimens were tested at different temperature and humidity levels to study the environmental effects on the creep behaviors. The viscoelastic behavior of vinylester resins under various environmental conditions was characterized and represented by a two-parameter Maxwell model, as shown in Equation (5). The material constants of vinylester resins obtained by the Maxwell model for two environmental conditions are listed in Table 1. Two laminates, $[(+45°/-45°/CSM)_2]_s$ and $[(90°/+45°/-45°/CSM)_3]_s$, were tested under tensile loads, and the comparisons of the predicted creep compliances with the experimental data are shown in Figures 3 through 6. The differences at 20 hours between experiments and proposed model by the power law fitting are about 1.0% (Figure 3) and 6.7% (Figure 4) for the $[(+45°/-45°/CSM)_2]_s$ laminates under two

Table 1. Material constants of vinylester resins by Maxwell model [14].

Environmental Conditions	E^M(GPa)	μ^M (GPa·hr)
21°C (70°F) and 12% RH*	3.86	855.09
66°C (150°F) and 80% RH*	2.62	165.99

*RH: relative humidity.

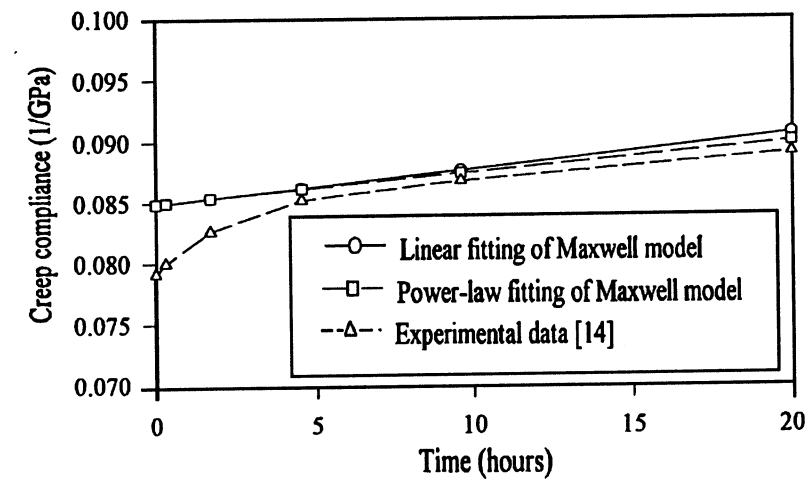

Figure 3. Creep compliance of laminate $[(+/-45°/CSM)_2]_s$ for 21°C and 12% RH.

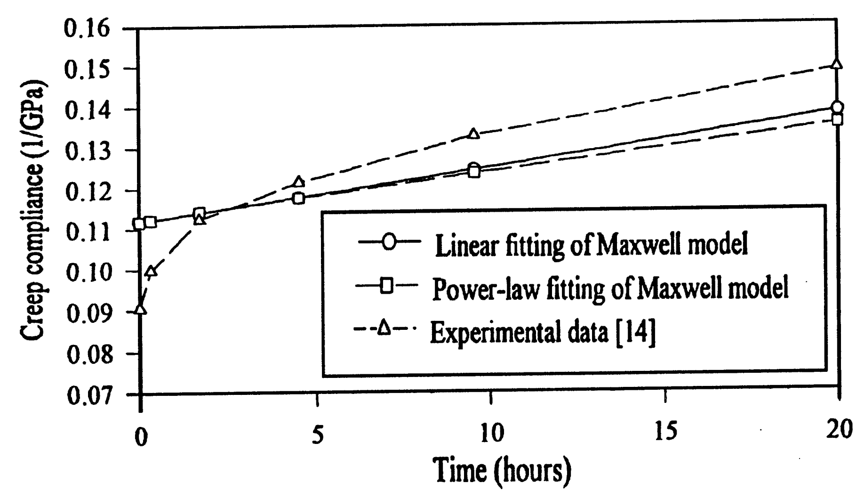

Figure 4. Creep compliance of laminate $[(+/-45°/CSM)_2]_s$ for 66°C and 80% RH.

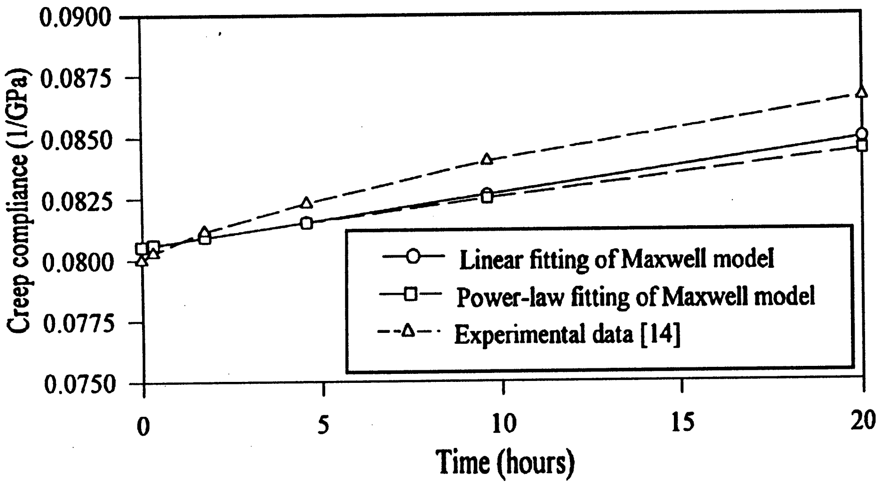

Figure 5. *Creep compliance of laminate [(90°/+/−45°/CSM)$_3$]$_s$ for 21°C and 12% RH.*

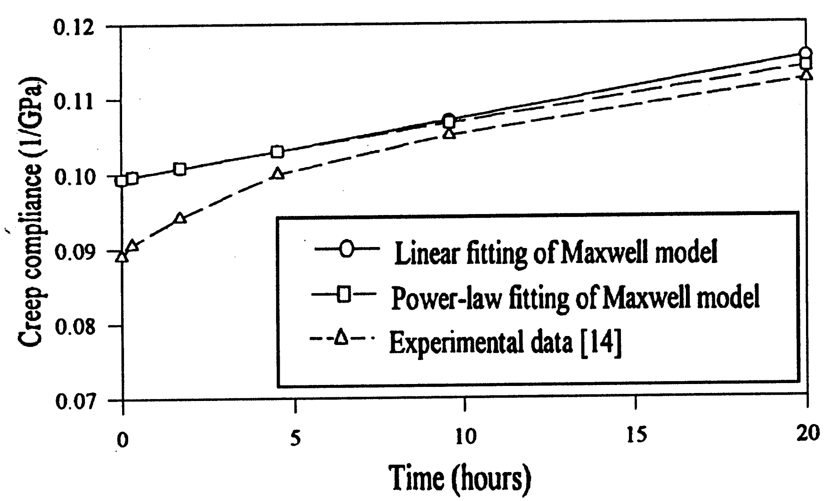

Figure 6. *Creep compliance of laminate [(90°/+/−45°/CSM)$_3$]$_s$ for 66°C and 80% RH.*

different conditions; whereas for the [(90°/+45°/−45°/CSM)$_3$]$_s$ laminates, the differences are 2.5% (Figure 5) and 1.5% (Figure 6), respectively. As shown in Figures 3–6, the proposed model can accurately predict the creep responses of laminates under tensile loads.

PARAMETRIC STUDY ON THE CREEP COMPLIANCES OF [+/−θ°]$_S$ LAMINATES

Since the resin or matrix is reinforced with fibers to resist in part creep deformations, the orientations of fiber reinforcement may have significant effects on the creep resistance of composite materials. FRP laminates with [+/−θ°]$_s$ lay-up configuration are used to demonstrated the influence of fiber orientations on their viscoelastic response. The laminate creep compliance coefficients (S_{ij}) versus the fiber orientation (θ) are plotted in Figure 7. As shown in Figure 7, the creep compliances S_{11} and S_{22} are antisymmetric to each other, and the curves also illustrate that the laminates have the lowest creep compliance (S_{66}) at θ = +/−45°, which implies that the [+/−45°]$_s$ laminates provide the best creep resistance under in-plane shear loading.

Viscoelastic Response of FRP Beams

To demonstrate the accuracy of the present model to predict flexural creep of beams, a pultruded FRP box-beam is tested under sustained loading over a 5-day period, and the experimental data are computed with the present model. Also, a study on the influence of fiber architectures on flexural creep of an FRP wide-flange beam is presented.

CREEP BEHAVIOR OF A GLASS FRP BOX-BEAM

A pultruded FRP box-beam manufactured by Creative Pultrusions, Inc., Alum Bank, PA is tested under bend loading, and its creep flexural behavior is evaluated by applying a sustained load over a 5-day period. The beam was tested at room temperature and relative humidity. The beam is simply supported with a span of 3.66 m (12.0 ft) and subjected to 1/3-span permanent point loads of 4.5 kN (1.0 kip) each. The box-beam, 101.6 × 101.6 × 6.35 mm (4" × 4" × 1/4"), is manufactured from E-glass fiber and vinylester resin, and each panel consists of two continuous strand mats and one unidirectional roving layer. Displacement transducers and strain gages are installed at the beam midspan section and transverse deflection and maximum compressive and tensile strains are recorded over time. The viscoelastic properties of vinylester resin used in the model are the same as those listed in Table 1. The results for deflections obtained with Equation (29) are compared to the experimental data (Figure 8). The differences for deflections between experimental and predicted values at 120 hrs are about 5.4% for linear fitting and negligible for power-law fitting of Maxwell models. For the maximum compressive strains at the beam midspan (Figure 9a), the percentage differences at 120 hrs

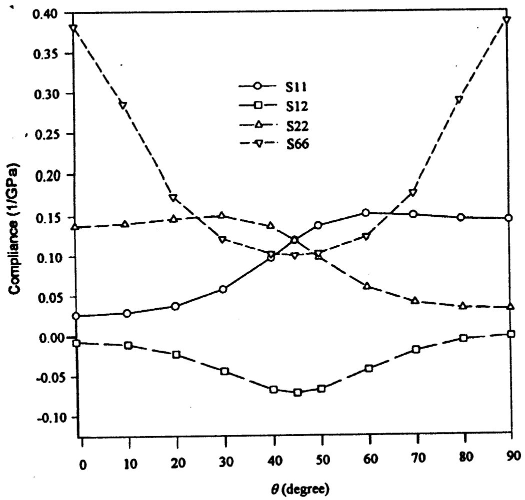

Figure 7. Creep compliance coefficients of $[+/-\theta]_s$ laminate.

are about 5.4% for linear fitting and 4.9% for power-law fitting of Maxwell models; while for the maximum tensile strain, the percentage differences are negligible (within 1.6%) for both fitting approaches of Maxwell models. As indicated in Figures 8 and 9, the model predictions correspond favorably to the experimental data.

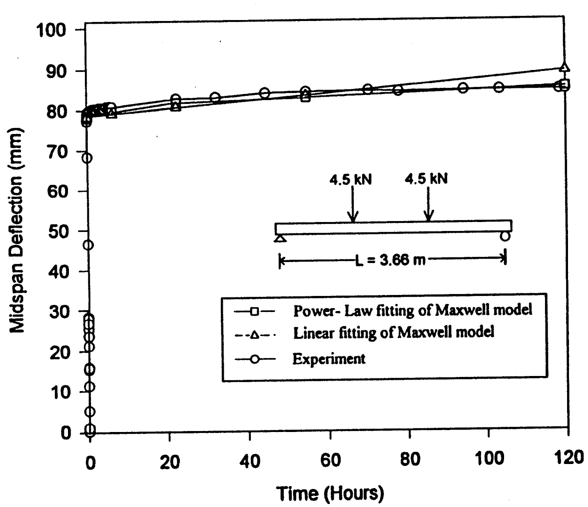

Figure 8. Midspan deflections for glass FRP box-beam.

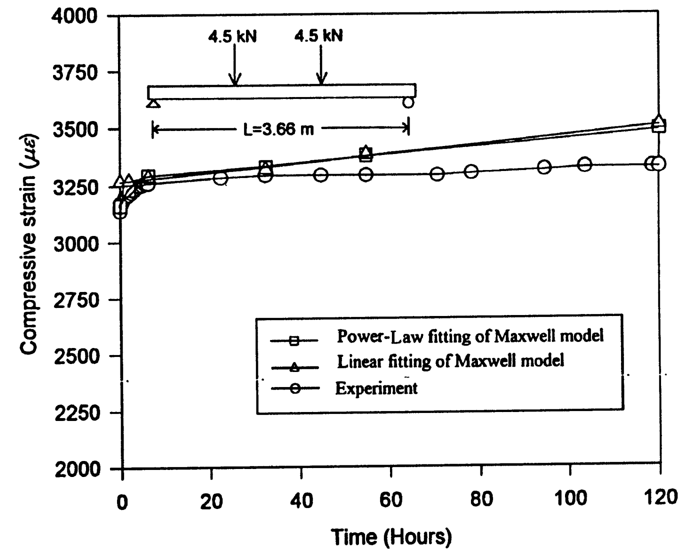

Figure 9a. Midspan compressive strains at the top flange for glass FRP box-beam.

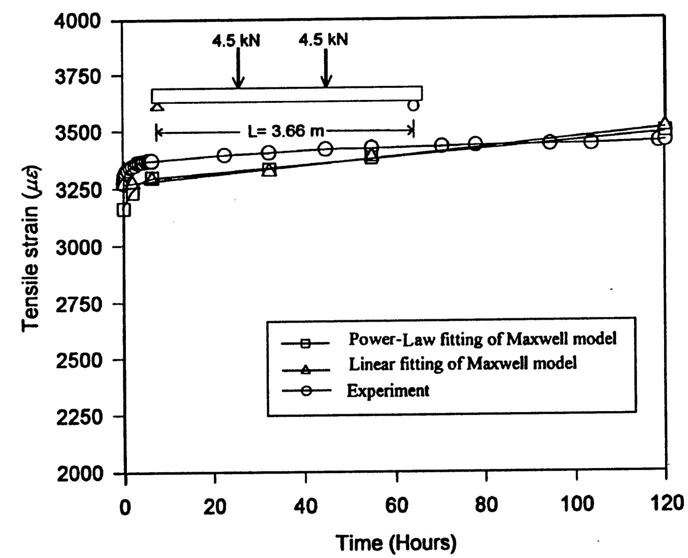

Figure 9b. Midspan tensile strains at the bottom flange for glass FRP box-beam.

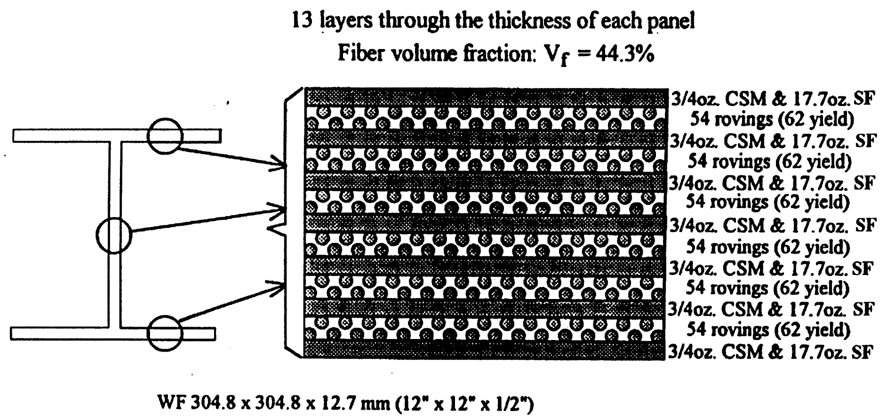

Figure 10. *Fiber architecture of FRP wide-flange beam.*

FLEXURAL CREEP OF FRP WIDE-FLANGE BEAMS UNDER BENDING

Since there is only limited information available in the literature, an analytical study on the viscoelastic behavior of thin-walled FRP wide-flange beams is carried out. First, the accuracy of the results is partially checked for the model made of only vinylester resin without reinforcing fibers ($V_f = 0$). Later, the trends of predictions with respect to certain parameters, such as fiber orientations and fiber volume fractions, are examined. The material properties of the vinylester matrix used in the model are those given in Table 1 for 21°C (70°F) temperature and 12% relative humidity.

Based on an optimized design [25], a Wide-Flange (WF) section [304.8 × 304.8 × 12.7 mm (12" × 12" × 1/2")] was produced by industry and tested in the elastic range. The section lay-up is shown in Figure 10, and the fiber percentages of CSM, SF, and roving layers are 5.0%, 13.0% and 26.3%, respectively. In Table 2, the measured mid-span maximum elastic deflections and strains compare well with the predicted elastic micro/macromechanics results [26,27].

Table 2. Elastic response comparisons for wide-flange beam.

Span Length	L = 3.66 m (12.0 ft)			
Loading	3-Point Bending		4-Point Bending	
Result Type	Experimental [26]	FRPBEAM [27]	Experimental [26]	FRPBEAM [27]
δ_{max} (mm/kN)	0.213	0.215	0.199	0.201
ϵ_{max} ($\mu\epsilon$/kN)	23.6	25.3	18.0	18.6

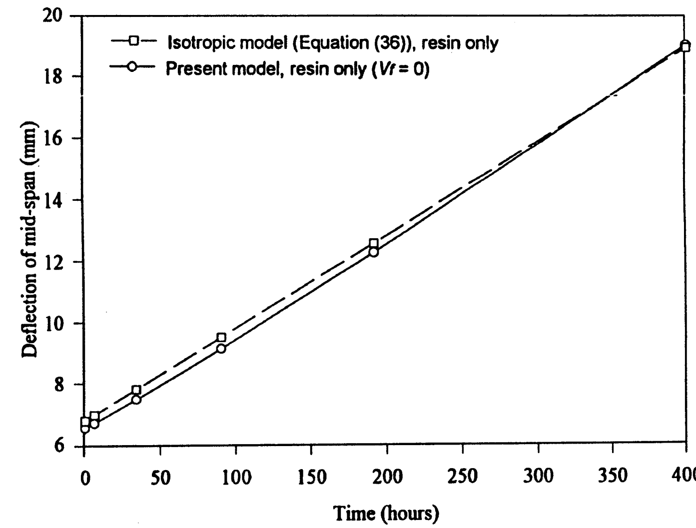

Figure 11. *Creep deflection versus time for beam with zero fiber volume fraction.*

To indirectly validate the proposed model for "isotropic" WF beams, the viscoelastic behavior of the beam shown in Figure 10 but composed of only vinylester resin ($V_f = 0$) is examined first. The beam can be considered to be isotropic, and its deflection under 3-point bending is

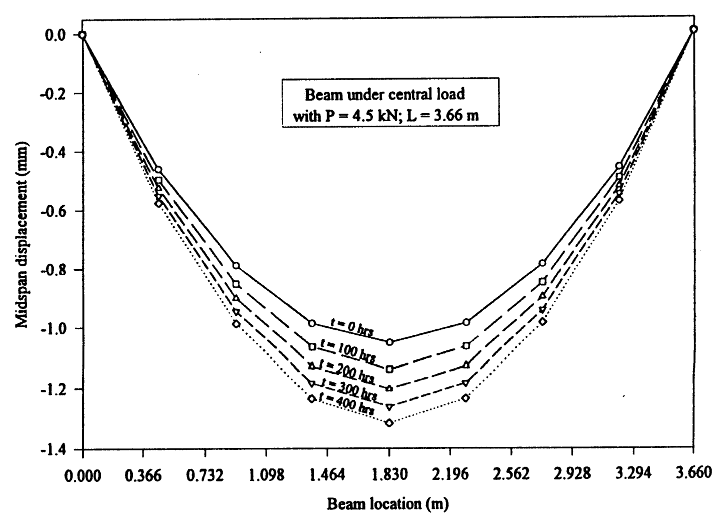

Figure 12. *Beam creep deflection profile with respect to time.*

$$\delta_{Total} = \delta_{Bending} + \delta_{Shear} = \frac{P_Y L^3}{48E^C I} + \frac{P_Y L}{4K_Y G^C A} \tag{36}$$

where $K_y \approx 1.0$; I and A are the geometric cross-sectional properties; and E^C and G^C are the relaxation moduli of matrix and obtained from the creep compliance of Equation (5). Assuming that the Poisson ratio of matrix ($\nu_0 = 0.35$) remains constant in the time domain, the moduli are:

$$E^C = L(t) = \frac{1}{M(t)}$$
$$G^C = \frac{L(t)}{2(1+\nu_0)} = \frac{1}{2M(t)(1+\nu_0)} \tag{37}$$

In Figure 11, the predicted creep deflections of the FRP WF beam modeled as isotropic through Equation (36) compare favorably with the values obtained from the present model for zero fiber-volume fracture.

Using the FRPCREEP program, the viscoelastic response of the WF beam shown in Figure 10 is characterized. The model is subjected to a central load P, and the beam length is $L = 3.66$ m (12.0 ft). Figure 12 shows the beam creep deflection profiles over time for $P = 4.5$ kN (1.0 kip). The linear viscoelastic responses of strains under different load levels are illustrated in Figure 13. The influence of SF material architecture on the beam viscoelastic behavior is analyzed next. The beam creep deflections for varying orientations (θ) of SF layers are plotted in Figures 14(a) and (b). After about 90 hours, the fiber orientation of SF layers around $\theta = 30°$ shows a better creep resistance [Figure 14(a)] and an approximate linear and stable creep displacement trend [Figure 14(b)]. Thus, when the orientation (θ) of SF layers is around 30°, the beam has the least creep deformations over time. The beams with $\theta = 0°$ orientation of SF layers show a better creep performance within a short time-range; however, as time increases, the creep deformations also increase quickly due to the increased shear creep deformations. The influence of fiber volume fractions (V_f) on the beam creep behavior is presented in Figure 15. As expected, the beam creep deflections have a stable variation over time for beams with high fiber volume fractions. Most practical pultruded sections have V_f values between 0.3 and 0.5.

CONCLUSIONS AND RECOMMENDATIONS

The model proposed in this study is used for predicting the creep flexural behavior of thin-walled laminated FRP beams. The formulas for creep deflections and

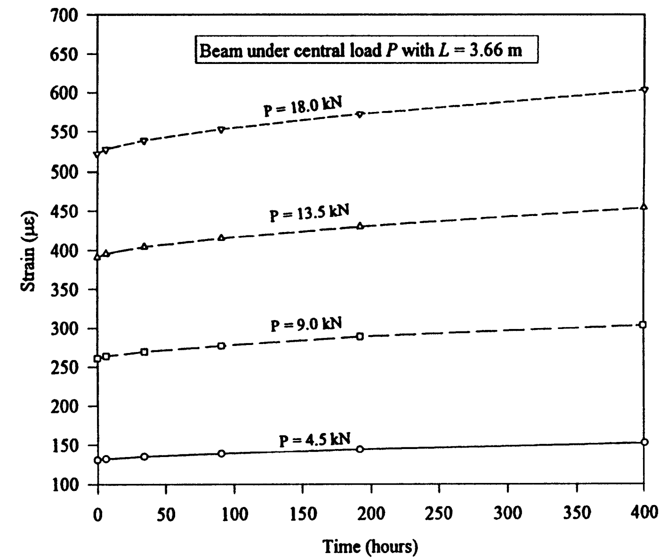

Figure 13. *Maximum creep tensile strains (ϵ_x) on the bottom flange of beam.*

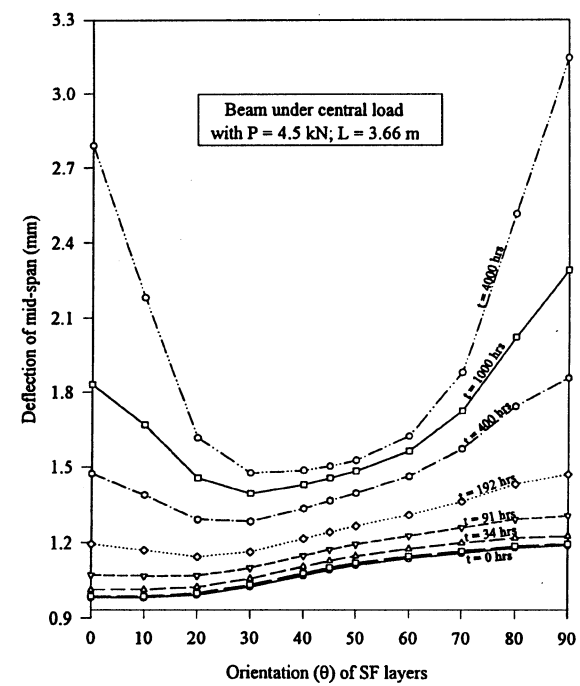

Figure 14a. *Beam creep deflection versus orientation (θ) of SF layers.*

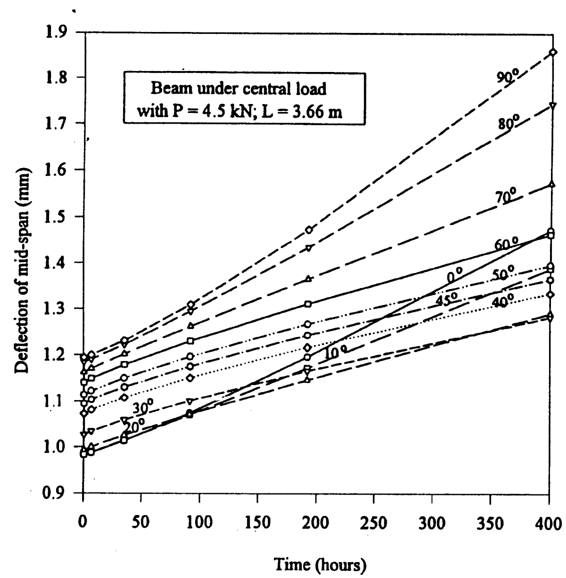

Figure 14b. Beam creep deflection versus orientation (θ) of SF layers.

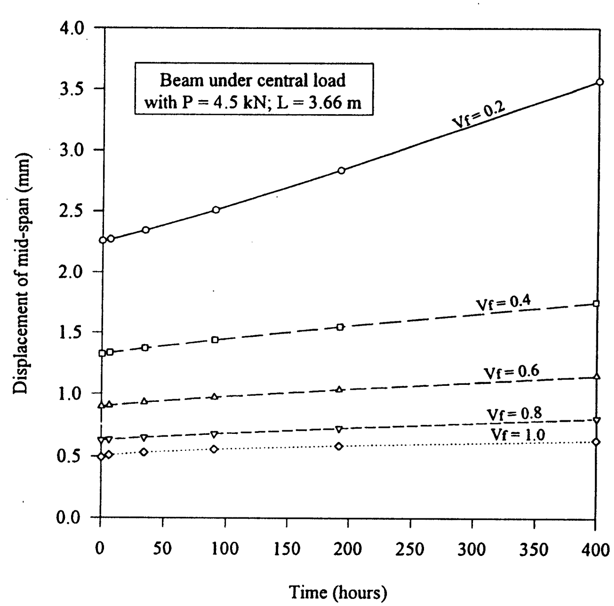

Figure 15. Beam creep deflection versus time with varying fiber volume fractions.

strains are derived in the Carson domain, and their corresponding numerical solutions in the time domain are presented. Good agreements with experimental data for both FRP laminates under tensile loads and a box-beam under bending load are obtained. The deflection predictions of the model for a wide-flange beam [304.8 × 304.8 × 12.7 mm (12" × 12" × 1/2")] manufactured only from vinylester resin compare well with those for an isotropic material model. The parametric study of the influence of material architecture and fiber volume fraction on the linear viscoelastic response of the wide-flange beams demonstrates the capability of the present model as an efficient tool for flexural creep analysis and design of FRP beams.

There is limited information in the literature on experimental flexural creep response of FRP beams, and therefore, experimental testing of creep behavior of various FRP beams in bending is needed to correlate results with the present model. In the present study, the environmental effects on the viscoelastic response of FRP beams are not considered. These effects, such as temperature and humidity, are significant in practical designs and can be further incorporated in the present model. These additional concerns need to be addressed in creep analysis of FRP beams, and the present model can be used as the basis for further work in this area.

ACKNOWLEDGMENT

The authors thank Creative Pultrusions, Inc. for producing the testing samples. This study was partially sponsored by the National Science Foundation under CRCD program (Grant No. EEC-9700772).

REFERENCES

1. Harris, J. S. and Barbero, E. J. 1998. "Prediction of Creep Properties of Laminated Composites from Matrix Creep Data." *J. of Reinforced Plastics and Composites,* 17(4):361–378.
2. Lee, O. and Ueng, C. E. S. 1995. "Creep Phenomenon of Simple Composite Structures." *J. of Composite Materials,* 29(15):2069–2089.
3. Holmes, M. and Al-Khayatt, S. 1975. "Structural Properties of GRP." *Composites,* 6(4):157–165.
4. Flugge, W. 1967. *Viscoelasticity.* Blaisdell Publishing Company, Waltham, MA.
5. Hashin, Z. 1965. "Viscoelastic Behavior of Heterogeneous Media." *ASME J. of Applied Mechanics,* 29(32):630–636.
6. Hashin, Z. 1966. "Viscoelastic Fiber Reinforced Materials." *AIAA J.,* 4:1411–1417.
7. Christensen, R. M. 1979. *Mechanics of Composite Materials.* John Wiley & Sons, New York, NY.
8. Laws, N. and McLaughlin, J. R. 1978. "Self-consistent Estimates for the Viscoelastic Creep Compliances of Composite Materials." *Proceedings of the Royal Society,* London, 39:251–273.
9. Wang, Y. M. and Weng, G. J. 1992. "The Influence of Inclusion Shape on the Overall Viscoelastic Behavior of Composites." *ASME J. of Applied Mechanics,* 59:510–518.
10. Barbero, E. J. and Luciano, R. 1995. "Micromechanical Formulas for the Relaxation Tensor of Linear Viscoelastic Composites with Transversely Isotropic Fibers." *Int. J. of Solids and Structures,* 32(13):1859–1872.

11. Luciano, R. and Barbero, E. J. 1995. "Analytical Expressions for the Relaxation Moduli of Linear Viscoelastic Composites with Periodic Microstructure." *Journal of Applied Mechanics*, ASME, 62(3):786–793.
12. Iwakuma, T. and Nemat-Nasser, S. 1983. "Composites with Periodic Microstructure." *Computers and Structures*, 16(1–4):13–19.
13. Luciano, R. and Barbero, E. J. 1994. "Formulas for the Stiffness of Composites with Periodic Microstructure." *Int. Journal of Solids and Structures*, 31(21):2933–2944.
14. Harris, J. S. 1996. *Environmental Effects on the Creep Response of Polymer Matrix Composites and Metal Matrix Composites*. Master of Science Thesis, West Virginia University, Morgantown, WV.
15. Barbero, E. J., Lopez-Anido, R. and Davalos, J. F. 1993. "On the Mechanics of Thin-walled Laminated Composite Beams." *J. Composite Materials*, 27:806–829.
16. Massa, J. C. and Barbero, E. J. 1998. "A Strength of Materials Formulations for Thin Walled Composite Beams with Torsion," *J. Composite Materials*, (17):1560–1594.
17. Barbero, E. J. 1999. *Introduction to Composite Materials Design*. Taylor & Francis, Philadelphia, PA.
18. Whitney, J. M., Browning, C. E. and Mair, A. 1974. "Analysis of the Flexure Test for Laminated Composite Materials." *Composite Materials: Testing and Design (3rd Conference)*, ASTM STP 546, ASTM, 30–45.
19. Tsai, S. W. 1988. *Composites Design*. Think Composites, Dayton, Ohio.
20. Davalos, J. F., Salim, H. A., Qiao, P., Lopez-Anido, R. and Barbero, E. J. 1996. "Analysis and Design of Pultruded FRP Shapes under Bending." *Composites: Part B, Engineering J.*, 27(3–4):295–305.
21. Aboudi, J. 1991. *Mechanics of Composite Materials, a Unified Micromechanical Approach*. Elsevier, New York.
22. Yancey, R. N. and Pindera, M. J. 1990. "Micromechanical Analysis of the Creep Response of Unidirectional Composites." *ASME J. of Engineering Materials and Technology*, 112:157–163.
23. Nemat-Nasser, S. and Taya, M. 1981. "On Effective Moduli of an Elastic Body Containing Periodically Distributed Voids." *Quarterly Applied Mathematics*, 39:43–59.
24. Hull, D. 1981. *An Introduction to Composite Materials*. Cambridge University Press.
25. Davalos, J. F., Qiao, P. and Barbero, E. J. 1996. "Multiobjective Material Architecture Optimization of Pultruded FRP I-beams." *Composite Structures*, 35(3):271–281.
26. Qiao, P. 1997. *Analysis and Design Optimization of Fiber-reinforced Plastic (FRP) Structural Beams*. Doctoral Dissertation, Department of Civil and Environmental Engineering, West Virginia University, Morgantown, WV.
27. Qiao, P., Davalos, J. F. and Barbero, E. J. 1994. *FRPBEAM: A Computer Program for Analysis and Design of FRP Beams*. Department of Civil and Environmental Engineering, West Virginia University, Morgantown, WV.

The Effective Friction Coefficient of a Laminate Composite, and Analysis of Pin-loaded Plates

YI XIAO,* WEN-XUE WANG AND YOSHIHIRO TAKAO
Research Institute for Applied Mechanics
Kyushu University
6-1 Kasuga-koen, Kasuga 816-8580, Japan

TAKASHI ISHIKAWA
Airframe Division
National Aerospace Laboratory
6-13-1 Ohsawa, Mitaka, Tokyo 181-0015, Japan

(Received October 20, 1998)
(Revised May 21, 1999)

ABSTRACT: A calculation method based on M-CLT (Modified Classical Lamination Theory) for the friction coefficient of a CFRP (Carbon Fiber Reinforced Plastic) composite laminate edge is proposed. It is derived based on experimental friction coefficients in unidirectional off-axis laminae and a high-order algebraic equation from a numerical solution to the specific boundary for the frictional contact problem. A numerical experiment of a frictional contact problem is also performed by means of a nonlinear three-dimensional finite element analysis and the results are compared with those obtained from the M-CLT method for various contact directions. Good agreement is found between the two sets of results. Finally, the friction coefficient derived by using the M-CLT method is applied to a two-dimensional contact stress analysis of a pin-loaded composite laminate. The effects of the method used to calculate the friction coefficient on the contact stress distribution are investigated.

KEY WORDS: CFRP laminate, friction coefficient, M-CLT method, pin-loaded composite laminate, contact stress.

*Author to whom correspondence should be addressed at Airframe Division, National Aerospace Laboratory, 6-13-1, Ohsawa, Mitaka, Tokyo 181-0015, Japan.

0021-9983/00/01 0069–19 $10.00/0